NASA TECHNICAL NOTE

NASA TN D-5089

SUMMARY AND CORRELATION OF SKIN-FRICTION AND HEAT-TRANSFER DATA FOR A HYPERSONIC TURBULENT BOUNDARY LAYER ON SIMPLE SHAPES

by Edward J. Hopkins, Morris W. Rubesin, Mamoru Inouye,
Earl R. Keener, George C. Mateer, and Thomas E. Polek

Ames Research Center
Moffett Field, Calif.

SUMMARY AND CORRELATION OF SKIN-FRICTION AND

HEAT-TRANSFER DATA FOR A HYPERSONIC

TURBULENT BOUNDARY LAYER

ON SIMPLE SHAPES

By Edward J. Hopkins, Morris W. Rubesin, Mamoru Inouye,
Earl R. Keener, George C. Mateer, and Thomas E. Polek

Ames Research Center
Moffett Field, Calif.

NATIONAL AERONAUTICS AND SPACE ADMINISTRATION

SUMMARY AND CORRELATION OF SKIN-FRICTION AND

HEAT-TRANSFER DATA FOR A HYPERSONIC

TURBULENT BOUNDARY LAYER

ON SIMPLE SHAPES[1]

By Edward J. Hopkins, Morris W. Rubesin, Mamoru Inouye,
Earl R. Keener, George C. Mateer, and Thomas E. Polek

Ames Research Center

SUMMARY

Local skin-friction and heat-transfer data were directly measured in air for turbulent boundary layers on flat plates, cones, and a wind-tunnel wall. The Mach number at the edge of the boundary layer ranged between 5 and 7.4 and the wall to adiabatic wall temperature ratio varied between 0.1 and 0.6.

The skin-friction and heat-transfer data are compared with other data obtained by direct measurement of surface shear with balances and accompanied by boundary-layer surveys. The use of momentum-thickness Reynolds number in the skin-friction comparison avoids the need for arbitrary location of the virtual origin of the turbulent boundary layer. A boundary-layer energy thickness obtained from integration of the heat-flux distribution up to a test station proved useful in correlating the local heat flux at that station in a manner analogous to the use of momentum thickness.

Adiabatic and cold wall data are employed to assess four theories for predicting turbulent skin friction. The theories examined are those of Sommer and Short, Spalding and Chi, Van Driest II, and Coles.

Analysis of the skin-friction data indicates that the theory of either Van Driest II or Coles gives the best predictions for wall to adiabatic wall temperature ratios above 0.3, generally within about ±10 percent of the measured values. Although Coles' theory gives results generally comparable to those of the Van Driest II theory, at high Reynolds numbers it underpredicts the results by more than 10 percent. At Mach numbers near 6 and above, theories of Sommer and Short or Spalding and Chi generally underpredict the measured skin friction by 20 to 30 percent. At wall to adiabatic wall temperature ratios below 0.3, none of the theories give the proper trend with wall to adiabatic wall temperature ratio.

The heat-transfer analysis for nonadiabatic conditions generally substantiates the skin-friction analysis, favoring the theory of either Van Driest II or Coles, provided the Reynolds analogy factor of 1.0 (containing an assumed recovery factor of 0.9) measured in the present investigation is employed.

---

[1]Presented at the "Symposium on Compressible Turbulent Boundary Layers," Langley Research Center, December 10-11, 1968.

INTRODUCTION

Accurate knowledge of skin friction and heat transfer is required to predict the performance and structural requirements of supersonic and hypersonic aircraft. Generally, calculations are relied upon to provide estimates of either wind-tunnel or flight values of skin friction since it is impractical to measure these values over the entire configuration. Similarly, the thermal design of airplane structures and the selection of material depend largely on predictions of the incoming convective heat flux over the various surface elements. Supersonic and hypersonic aircraft will operate with skin temperatures near the radiative equilibrium temperature, where the incoming convection is balanced by radiation to the surroundings. At supersonic speeds ($M \simeq 3$), the radiation equilibrium temperature is almost equal to the adiabatic wall temperature. At hypersonic speeds ($M \simeq 7$), however, the external surfaces will generally have wall to adiabatic wall temperature ratios between 0.3 and 0.5 as a result of considerable radiative cooling and internal heat transfer.

Previous evaluations of turbulent skin-friction theories may have questionable accuracy at hypersonic Mach numbers for lack of many direct measurements by skin-friction balances. These evaluations include numerous indirect measurements from (1) heat transfer with an assumed Reynolds analogy factor, (2) rate of change of momentum thickness with longitudinal distance, (3) velocity gradient at the surface, or (4) velocity profile. Examples of such evaluations are those of Spalding and Chi (ref. 1), Hopkins and Keener (ref. 2) and Peterson (ref. 3). Spalding and Chi examined 20 theories and showed that the theories of Van Driest II (ref. 4) and Sommer and Short (ref. 5) gave root-mean-square deviations of about 11 and 14 percent respectively compared with 10 percent for their semi-empirical theory. Independent studies of references 2 and 3 indicate that for the adiabatic-wall case the theories of Van Driest II and Sommer and Short bracket nearly all the experimental results. For the non-adiabatic wall case, Peterson's analysis also favors Sommer and Short's theory up to a Mach number of 6. Miles and Kim (ref. 6) show that Coles' theory, not considered in the other analyses, is competitive with Spalding and Chi's theory for the nonadiabatic wall case.

Heat-transfer data for flat plates are compared by Bertram et al. (refs. 8 and 9) with theoretical values derived from skin-friction theory through an extension to compressible flow of the von Kármán form of the Reynolds analogy factor. Bertram's analysis and later results of Cary (ref. 10) suggest best agreement with the prediction method of Spalding and Chi.

Recently, a skin-friction balance became available that can be used on models in hypersonic facilities with elevated stagnation temperatures. However, preliminary skin-friction measurements at Mach number 6.5 were not in accord with the cited heat-transfer results in indicating the best theory for predictions. Consequently, the present investigation was undertaken to obtain both heat-transfer measurements on flat plates and cones and skin-friction measurements on flat plates and a wind-tunnel wall, all surfaces being nonadiabatic. This investigation was conducted in the Ames 3.5-Foot Hypersonic Wind

Tunnel at Mach numbers between 5 and 7.5. Skin friction and heat transfer
were measured simultaneously at one of the longitudinal stations on a flat
plate to determine the Reynolds analogy factor. The results were then
employed to reevaluate the theories of Sommer and Short (ref. 5), Spalding and
Chi (ref. 1), Van Driest II (ref. 4), and Coles (ref. 7).

<div align="center">NOTATION</div>

C_f local skin-friction coefficient, $\dfrac{\tau}{q_e}$

C_F average skin-friction coefficient, $\dfrac{2\theta}{x}$ for a flat plate

C_h local Stanton number, $\dfrac{\dot{q}_w}{\rho_e U_e (H_w - H_{aw})}$

F_c transformation function for $C_f (\bar{C}_f = F_c C_f)$, reference 1

H total enthalpy

M Mach number

p pressure

Pr Prandtl number

q dynamic pressure

$\dot{q}_w$ rate of heat transfer from the surface per unit area

r local-cone radius, wind-tunnel radius, or temperature recovery factor

$R_{e,x}$ Reynolds number based on distance to virtual origin of turbulent flow, $\dfrac{\rho_e U_e x}{\mu_e}$

$R_{e,\Gamma}$ Reynolds number based on energy thickness, $\dfrac{\rho_e U_e \Gamma}{\mu_e}$

$R_{e,\theta}$ Reynolds number based on momentum thickness, $\dfrac{\rho_e U_e \theta}{\mu_e}$

s   distance along surface from cone apex or flat-plate leading edge

T   absolute temperature

U   velocity

x   distance along surface from either leading edge or virtual origin

x_L distance along surface from leading edge to peak Stanton number location

x_T distance along surface from virtual origin of turbulent flow to peak Stanton number location

y   distance normal to surface

α angle of attack

Γ energy thickness $\displaystyle\int_0^\delta \frac{\rho U}{\rho_e U_e}\left(\frac{H - H_e}{H_w - H_e}\right)dy$, also see equation (6)

δ boundary-layer thickness

θ momentum thickness $\displaystyle\int_0^\delta \frac{\rho U}{\rho_e U_e}\left(1 - \frac{U}{U_e}\right)dy$ for flat plates or

$$\int_0^\delta \frac{\rho U}{\rho_e U_e}\left(1 - \frac{U}{U_e}\right)\left(\frac{r - y}{r}\right)dy \quad \text{for circular wind-tunnel walls}$$

μ coefficient of viscosity

ρ mass density

τ shear stress

$(\bar{\ })$ variable transformed to equivalent constant property case

<center>Subscripts</center>

aw   adiabatic wall

e   boundary-layer edge

exp   experimental

i   incompressible

l   local station

L   laminar

max   maximum

t   total

T   turbulent

the   theoretical

w   wall

Superscript

ϵ index ($\epsilon = 0$ for flat plate and $\epsilon = 1$ for cone)

APPARATUS AND TEST

Wind Tunnel

The experimental investigation was conducted in air in the Ames 3.5-Foot Hypersonic Wind Tunnel. This facility is a "blow-down" type wind tunnel in which the air is heated by a hot pebble bed to temperatures ranging from about 1000° to 2100° R. The throat and nozzle walls are cooled by helium injection ahead of the throat, the helium remaining within the wind-tunnel boundary layer as confirmed by surveys. The Mach number 5.4 and 7.4 contoured nozzles were used, and the stagnation pressure was varied from about 7 to 120 atmospheres. The present tests used both a quick-insert mechanism and a fixed-support system for holding models.

Models and Instrumentation

Flat plates.- Two flat plates, 18 inches wide by 47 inches long, were tested. The leading edge of each plate was 0.004 inch thick and was unswept. Both flat plates were used to obtain skin friction and momentum thickness at a station 39 inches from the leading edge under nearly isothermal wall conditions. The first flat plate was sting supported with the test surface at an angle of 3° windward to the airstream. Both pitot-pressure and total-temperature boundary-layer profiles were obtained at the skin-friction test station. The second flat plate was mounted on the injection mechanism to obtain heat-transfer distributions on the surface. Thin-skin heat-transfer gages were installed in the heavy-walled steel plate along the centerline and also off center at several locations. Pitot-pressure profiles and skin friction were measured at the station 39 inches from the leading edge. This plate

was tested at angles of 0° and 3.1° windward to the airstream. Cross flow was minimized by fences 1 inch high at the trailing edge and tapering to zero at the leading edge.

Cones.- The conical heat-transfer models had half-angles of 5° and 15° and surface lengths of approximately 28 and 20 inches, respectively. These models were of thin-walled (0.033 in.) electroformed nickel and instrumented with thermocouples spot-welded to the interior surface. The 5° cone had a single row of 22 thermocouples spaced at 1-inch intervals along one conical ray. Tip radii were 0.005 and 0.0025 inch for the 5° and 15° models, respectively.

The wall-to-recovery-temperature ratio was varied by changing both the total temperature and the wall temperature. The preinjection value of the wall temperature was either the ambient value or 160° R. The latter value was obtained by externally cooling the model with liquid nitrogen before the model was injected into the airstream.

Test-section wall.- Skin-friction measurements and surveys of pitot pressure and total temperature were made on the test-section wall in the region of zero axial pressure gradient 27.5 feet from the nozzle throat and 8.5 feet behind the beginning of the test section. The local Mach number was 7.4 at the edge of the 8-inch-thick boundary layer. Normally, helium is injected ahead of the throat to cool the throat and the nozzle walls. During this test, however, the helium was shut off for periods up to 30 seconds while data were obtained with an air boundary layer. Five triple-shielded thermocouple total-temperature probes were used to survey the boundary layer at heights from 1 to 14 inches from the wall.

Skin-friction balance.- The skin friction was directly measured with floating-element balances manufactured by the Kistler Instrument Corporation. Four different balances were used, one at a time. The first measurement was made on the sting-mounted stationary flat plate with a balance having a 0.370-inch element diameter. Two balances, each 0.500 inch in diameter, were used consecutively with the injected flat plate. A fourth balance, 0.500 inch in diameter and contoured to fit the curved surface of the wind tunnel, was used in the test-section wall. The statically balanced elements of each balance were self-nulling to the center position with a perimetrical gap of 0.003 inch. The current required to produce the nulling force was calibrated against known weights. Electrical components were maintained at temperatures below 200° F by a water jacket. A test coil in the gage was used to simulate an external friction force and to check the calibration between each test run.

DATA REDUCTION

Flat Plates and Cones

Local flow conditions were calculated from the measured free-stream conditions for a two-dimensional wedge and a cone. Compressible flow relations were used in the calculations, including corrections for real gas

effects for calorically imperfect, thermally perfect air. Momentum thicknesses of the boundary layers on the flat plates were calculated from both the pitot-pressure profiles and an assumed Crocco linear total-temperature distribution with velocity (Pr = 1), which was found to agree with the measured total-temperature distributions. Energy thicknesses were obtained by integration of the measured heat-transfer rate along the plate. Viscosity was calculated by Keyes' equation.[2]

Test-section-wall data reduction was similar to that for the flat plates, except that the measured total-temperature profile was used in the calculations.

ACCURACY

The estimated probable uncertainties of the pertinent recorded and calculated quantities are as follows:

Free-stream p_t	±1 percent
Free-stream T_t	±50° R
Free-stream flow angle	±0.2°
Local flow angle	±0.3°
τ_w	±5 percent
T_w	±10° R
p_e	±5 percent
M_e	±0.17
q_e	±2 percent
$\rho_e U_e / \mu_e$	±7 percent
$R_{e,\theta}$ or $R_{e,\Gamma}$	±8 percent
Pitot-probe pressure	±2 percent
Boundary-layer total temperature	±50° R
y	±0.005 in.
θ or Γ	±5 percent
$\dot{q}_w$	±5 percent

DISCUSSION OF RESULTS

Skin Friction

The skin-friction data obtained in these tests at cold-wall conditions are summarized in tables I and II. The flat-plate data were obtained with and without boundary-layer trips. Because the data are in the form $C_f(R_{e,\theta})$, there is no need to define a virtual origin of turbulent boundary-layer flow in the analysis of the data.

[2]See note in Journal of Spacecraft and Rockets, vol. 4, no. 2, Feb. 1967, pp. 287-288 by Mitchel H. Bertram entitled "Comment on 'Viscosity of Air'."

An evaluation of the representative theories[3] of Sommer and Short (ref. 5), Spalding and Chi (ref. 1), Van Driest II (ref. 4), and Coles (ref. 7) for local turbulent skin friction is made by comparing the difference between experimental and theoretical skin friction for specified free-stream conditions and surface temperature. Most of the data was taken in the moderate Reynolds number range, $3 \times 10^3 < R_{e,\theta} < 30 \times 10^3$. Data taken at higher Reynolds numbers will be marked by high flags, data at lower Reynolds numbers by low flags. Adiabatic and nonadiabatic data are treated separately to discern the effects of Mach number and wall temperature independently. In addition, nonadiabatic wind-tunnel-wall data are treated separately from flat-plate data for reasons to be discussed.

Adiabatic wall.- Only existing skin-friction data for which both C_f and $R_{e,\theta}$ were directly measured in an airstream were chosen for the comparisons[4] presented in figure 1. Some of these adiabatic-wall data were taken in the constant-pressure regions on wind-tunnel walls instead of flat plates; however, contrary to the nonadiabatic data, the wall data are not believed to limit the evaluation because the momentum-thickness Reynolds number is relatively unaffected by differences in temperature distribution (ref. 11). The data are from references 2 and 12 through 19.

Comparisons presented in figure 1 indicate that at Mach numbers below 4 all the theories give about the same prediction for the data obtained at low and moderate Reynolds numbers ($R_{e,\theta} < 30 \times 10^3$). At high Reynolds numbers ($R_{e,\theta} > 30 \times 10^3$), however, Coles' theory tends to underpredict the experimental results by 10 to 15 percent. This Reynolds number effect in Coles' theory is related to the Reynolds number dependence of the temperature computed from the substructure hypothesis. As the Mach number is increased above 4, there is a tendency for the theories of Spalding and Chi and Sommer and Short to underpredict the data, reaching underpredictions of 20 and 30 percent, respectively, for Korkegi's data (ref. 19) near Mach number 6. Theories of Van Driest II and Coles predict the data within about 8 percent at the higher Mach numbers.

Nonadiabatic wall - flat plates.- Only skin-friction data for which C_f was directly measured on flat plates or circular cylinders (representative of flat plates) at Mach numbers between 5.6 and 7.4 were used in the comparisons presented in figure 2. The dashed lines represent fairings through the data, which include the unpublished data from Ames Research Center and the data from references 5 and 19 through 21. Sommer and Short (ref. 5) obtained their data from hollow circular cylinder models fired down a ballistic range. The local skin friction was calculated from the average skin friction of reference 5 by

---

[3]The transformed values of measured $R_{e,\theta}$ as given by each theory were used in the incompressible Kármán-Schoenherr equation of $\bar{C}_f$ as a function of $\bar{R}_{e,\theta}$ (ref. 2) to calculate the theoretical values of C_f. For Van Driest's theory, a temperature recovery factor of 0.9 was assumed in a manner similar to Spalding-Chi (ref. 1).

[4]Each symbol in figure 1 stands for a representative average of several data points taken over a limited Reynolds number range at the particular Mach number of a given experiment.

assuming that $C_f/C_{f,i} = C_F/C_{F,i}$. The analysis of Ames and Korkegi's data was based on the measured momentum-thickness Reynolds number; therefore, it was not necessary to derive a virtual origin of turbulent flow for these data. Examination of the Ames data indicates that any effect of boundary-layer trips on $C_f(R_{e,\theta})$ was within the experimental accuracy (compare the open circles with the solid circles). In addition, the results from the injected model (flagged solid symbols) agree with those for the stationary model (solid symbols).

The effect of two different choices for virtual origin of turbulent flow is also shown in figure 2. Theoretical local skin-friction coefficients for the data of Wallace and McLaughlin (ref. 21) and of Neal (ref. 20), for which the momentum-thickness Reynolds number was not measured, were calculated for Reynolds numbers obtained by two current methods for determining the virtual origin of turbulent flow. In the first method, the virtual origin was taken to be located at the position of maximum Stanton number (dashed symbols). In the second method, the virtual origin was derived by assuming that the momentum thickness for turbulent and laminar flow at the end of transition is equal $(x_T)(C_{F,T}) = (x_L)(C_{F,L})$, for which x_L was taken at the point where the Stanton number was maximum (regular symbols). Results from this latter method for Neal's data appear to be in better agreement with the Ames data.

For $T_w/T_{aw} > 0.3$, the theories of Van Driest II and Coles predict the skin friction within about 10 percent, whereas theories of Spalding and Chi and Sommer and Short underpredict the skin friction by 20 to 30 percent. At the lower temperature ratios, none of the theories predict the experimental variation of skin friction with wall to adiabatic wall temperature ratio.

Nonadiabatic wall - tunnel walls.- Measurements of nonadiabatic skin friction on wind-tunnel walls are treated separately because of the significant difference in measured temperature distributions presented in figure 3. For the flat plate, the Crocco linear temperature distribution (Pr = 1.0) as a function of velocity ratio represents the data, but for the tunnel side wall, the results lie closer to a quadratic temperature distribution. A similar difference between the temperature distributions on free-flight models and on a nozzle wall was noticed previously by Seiff and Short (ref. 22). They suggested that the history of the rapid expansion in the nozzle to high Mach numbers results in a boundary layer that is not in equilibrium with the local edge conditions.

The wind-tunnel-wall skin-friction data for $dp/dx \simeq 0$ are compared with predicted values based on flat-plate theory in figure 4. Note that the theories of Spalding and Chi, Van Driest II, and Coles are based on the Crocco linear temperature distribution; however, the data reflect the side-wall boundary-layer temperature distributions indicated in figure 3. In general, figure 4 shows that the theories of Sommer and Short, Spalding and Chi, and Van Driest II give about the same ratios of $(C_f)_{exp}/(C_f)_{the}$ at $T_w/T_{aw} \simeq 0.4$ on the wind-tunnel wall as on the flat plates (dashed lines). Coles' theory predicts these ratios from 20 to 30 percent below the data at $T_w/T_{aw} > 0.3$ (similar to the high Reynolds number data in fig. 1), which further indicates

that Coles' theory might be inherently incorrect at the higher Reynolds numbers. Wallace's data from two separate tests appear to be self-consistent within about ±10 percent and generally agree with the Ames data at $T_w/T_{aw} \simeq 0.3$. It is interesting that a flat-plate theory (in this case, Van Driest II) correlates the wall data at $T_w/T_{aw} > 0.3$.

<div align="center">Heat Transfer</div>

The analysis of the heat-transfer data parallels that for skin friction where it was found that expressing the data as

$$C_f = f(R_{e,\theta}, M_e, T_w/T_{aw}) \tag{1}$$

was useful in eliminating an arbitrarily assigned origin for the turbulent boundary layer. The local skin-friction coefficient is related to the momentum thickness and length Reynolds numbers by the momentum-integral equation

$$\frac{C_f}{2} \equiv \frac{\tau_w}{\rho_e U_e^2} = \frac{dR_{e,\theta}}{dR_{e,s}} + \frac{R_{e,\theta}}{r^\varepsilon} \frac{dr^\varepsilon}{dR_{e,s}} \tag{2}$$

where $\varepsilon = 0$ for a flat plate, $\varepsilon = 1$ for a cone, and the momentum thickness is defined as

$$\theta \equiv \int_0^\delta \frac{\rho U}{\rho_e U_e} \left(1 - \frac{U}{U_e}\right) dy \tag{3}$$

The results of boundary-layer pitot and total temperature surveys were introduced into equation (3) to evaluate the momentum thickness in the skin-friction analysis.

In an analogous manner, the local Stanton number is related to the energy thickness and length Reynolds numbers by the energy-integral equation $(H_w = \text{const})$

$$C_h \left(\frac{H_w - H_{aw}}{H_w - H_e}\right) \equiv \frac{\dot{q}_w}{\rho_e U_e (H_w - H_e)} = \frac{dR_{e,\Gamma}}{dR_{e,s}} + \frac{R_{e,\Gamma}}{r^\varepsilon} \frac{dr^\varepsilon}{dR_{e,s}} \tag{4}$$

where the energy thickness is defined as

$$\Gamma \equiv \int_0^\delta \frac{\rho U}{\rho_e U_e} \left(\frac{H - H_e}{H_w - H_e}\right) dy \tag{5}$$

Instead of boundary-layer surveys, the local heat-flux distribution was employed to evaluate Γ from

$$\Gamma = \frac{\int_0^{S_1} \dot{q}_w(s) r^\varepsilon(s)\,ds}{\rho_e U_e (H_w - H_e) r_1^\varepsilon} \qquad (6)$$

which results from the integration of equation (4). In the evaluation of equation (6), the boundary layer ahead of the first thermocouple station was assumed laminar with $\dot{q}_w \sim s^{-1/2}$. In a few tests in which both boundary-layer surveys and heat-flux distributions were obtained, it was found that Γ from equations (5) and (6) agreed within 7 percent.

Prediction of turbulent-boundary-layer heat transfer from skin-friction theories, $C_f(R_{e,\theta})$, requires the assumption of a Reynolds analogy factor and a recovery factor. Choices for these factors are based either on extensions of the now classic constant-property theories or on past experimental results. If these quantities are uniform along the surface, C_h and $C_f/2$, and $R_{e,\Gamma}$ and $R_{e,\theta}$ are related as follows:

$$(C_h)_{the} = \left(\frac{C_h}{C_f/2}\right)\left(\frac{C_f}{2}\right)_{the}$$

$$R_{e,\theta} = \frac{R_{e,\Gamma}}{\left(\dfrac{C_h}{C_f/2}\right)\left(\dfrac{H_w - H_{aw}}{H_w - H_e}\right)}$$

where $C_h/(C_f/2)$ is the Reynolds analogy factor, and r, the recovery factor, is introduced into the adiabatic wall enthalpy

$$H_{aw} = H_e - (1 - r)\frac{U_e^2}{2}$$

Typical variations of C_h with $R_{e,\Gamma}$ for a $5°$ cone and a flat plate with nearly the same conditions of M_e and T_w/T_{aw} are shown in figure 5. A recovery factor of 0.85 was used for laminar flow and 0.9 for turbulent flow, with a linear interpolation in the transition region. Although the transition location differs for the two shapes, the Stanton number for the fully turbulent flow is essentially the same for a given value of $R_{e,\Gamma}$.

The heat-transfer results are presented in figure 6 in a form analogous to the skin friction (see fig. 2(b)). Shown are recent Ames data for $5 < M_e < 7.4$ obtained on two cones with a wall-temperature-ratio range of $0.11 < T_w/T_{aw} < 0.6$ and on a flat plate with $T_w/T_{aw} \simeq 0.3$. To relate the heat-transfer results to the skin-friction theories, either as $(\dot{q}_w)_{exp}/(\dot{q}_w)_{the}$ or $(C_h)_{exp}/(C_h)_{the}$, it is necessary to assume values for the recovery and Reynolds analogy factors. For figure 6, the values assumed are $r = 0.9$ and $C_h/(C_f/2) = 1.16$, which are characteristic of supersonic flow and

11

moderate cooling rates. From these results, it would be concluded that the Spalding and Chi theory agrees best with the experimental results. This conclusion, however, is inconsistent with the findings of the skin-friction data, where the Van Driest II and Coles theories are favored. Thus, the skin-friction and heat-transfer experiments lead to different conclusions regarding the accuracy of prediction theories, at least when the usually accepted values of $r = 0.9$ and $C_h/(C_f/2) = 1.16$ are used.

To reconcile the dichotomy between the skin-friction and heat-transfer results, a short series of tests was conducted in which simultaneous measurements were made of local heat flux and skin friction on a flat plate with $T_w/T_{aw} \approx 0.3$. It was found that the heat flux shear ratio, $\dot{q}_w U_e/[\tau_w(H_w - H_e)]$, varied between 0.84 and 0.94, depending on the Reynolds number, whereas, at this wall temperature, the ratio calculated for $r = 0.9$ and $C_h/(C_f/2) = 1.16$ is 1.02. Furthermore, substituting $Pr = 0.72$ and $Pr_T = 1.0$ into the von Kármán Reynolds analogy factor and the corresponding recovery factor expression by Van Driest resulted in a heat flux shear ratio of 1.06 over the Reynolds number range of the tests. Thus, for the conditions of these tests, there is about a 10 to 20 percent reduction in heat transfer relative to skin friction from values expected from past experiments and theory. The data are too limited to permit evaluating the Reynolds analogy and recovery factors individually from the measured heat flux shear ratios. Therefore, it is necessary to rely on theory or a hypothesis to distinguish the effects of each factor. The von Kármán Reynolds analogy and Van Driest recovery factor expressions can be forced to agree with the heat flux shear ratio data by imposing a turbulent Prandtl number of 0.7 and arriving at $r = 0.7$ and $C_h/(C_f/2) = 1.4$. Alternatively, as shown in figure 7, the hypothesis that the recovery factor remains equal to 0.9 requires that $C_h/(C_f/2) \approx 1.0$, which is 15 to 20 percent lower than the value usually employed. This is illustrated by the dashed line, which represents the von Kármán Reynolds analogy factor ($Pr \approx 0.725$, $Pr_T = 1.0$) extended to compressible flows (ref. 8).

To test the surface temperature range where the preceding values of r and $C_h/(C_f/2)$ remain valid, the data cited in figure 8(a) were analyzed with $r = 0.7$, $C_h/(C_f/2) = 1.4$ and with $r = 0.9$, $C_h/(C_f/2) = 1$. It was found that the latter set of values caused the heat-transfer data (open symbols) to be more consistent with the skin-friction data (solid symbols) over the entire wall-temperature range shown in figure 8(b). With $r = 0.9$ and $C_h/(C_f/2) = 1$, the theories of Van Driest II and Coles predict the heat flux to within ± 10 percent at $T_w > 0.3T_{aw}$. The Spalding and Chi method generally underpredicted the heat-transfer data by 20 percent over the entire wall-temperature range.

CONCLUDING REMARKS

The turbulent boundary-layer skin-friction theories of Sommer and Short, Spalding and Chi, Van Driest II, and Coles have been evaluated on the basis

of directly measured skin friction on flat plates and wind-tunnel side walls. The use of momentum-thickness Reynolds number in the skin-friction comparisons avoids the need for arbitrarily locating the virtual origin of the turbulent boundary layer. At Mach numbers below 4, all the theories agree well with adiabatic wall data. On flat plates, at Mach numbers between 5.5 and 7.5 and wall to adiabatic wall temperature ratios down to 0.3, theories of Van Driest II and Coles give the best skin-friction predictions. For these temperatures, the theories of Sommer and Short or Spalding and Chi underpredict the skin friction by 20 to 30 percent. At lower wall temperatures, none of the theories gives the proper effect of wall-temperature level on the skin friction; however, the amount of data available is quite limited.

For the fully turbulent portions of the boundary layer on a wind-tunnel side wall at reduced temperatures, measured total temperature distributions were more nearly quadratic than linear with velocity as is characteristic of boundary layers on flat plates. This reflects the growth of the boundary layer in a favorable pressure gradient upstream of the test station. Even with these effects, when the measured profiles are used to evaluate the local momentum-thickness Reynolds number, values of $C_f(R_{e,\theta})$ on the side wall agree fairly well with the Van Driest II flat-plate theory.

The above theories have also been evaluated on the basis of heat-transfer measurements on cones and flat plates with boundary-layer-edge Mach numbers between 5 and 7.5 and wall to adiabatic wall temperature ratios between 0.1 and 0.6. A boundary-layer energy thickness obtained from integration of the heat-flux distribution up to a test station proved useful in correlating the local heat flux at that station, in a manner analogous to the use of momentum thickness. The theory of Spalding and Chi was in best agreement with the data, provided values of recovery factor equal to 0.9 and Reynolds analogy factor equal to 1.16 were used. Simultaneous measurements of heat transfer and skin friction on a flat plate at a single temperature ($T_w/T_{aw} = 0.3$) yielded heat flux shear ratios about 10 to 20 percent lower than the usually predicted values, the Reynolds analogy factor being unity if the recovery factor is assumed to remain constant at 0.9. Use of these values in the heat-transfer predictions at wall-temperature ratios between 0.2 and 0.8 produced results consistent with the skin-friction data. For wall to adiabatic wall temperature ratios greater than 0.3, the theories of Van Driest II and Coles predicted the heat-transfer data within ±10 percent. The theory of Spalding and Chi generally underpredicted the heat-transfer data by 20 percent over the complete wall-temperature range.

Although the assumptions cited in the previous paragraph caused the comparisons between heat-transfer data and theories to be consistent with those for skin friction, caution should be exercised in generalizing the results beyond the range of variables of this investigation. Turbulent-boundary-layer theory that admits changes in the Reynolds analogy factor invariably requires a change in the recovery factor. It was found that ignoring the latter change yielded the best correlation of the present data. Additional simultaneous heat-transfer and skin-friction data over a large range of surface temperatures are needed to distinguish the individual behavior of the Reynolds analogy and recovery factors as Mach number is increased and the

walls are highly cooled. Further, an understanding of these effects will require careful probing of the boundary layer to establish the distribution of quantities such as the turbulent Prandtl number.

REFERENCES

1. Spalding, D. B.; and Chi, S. W.: The Drag of a Compressible Turbulent Boundary Layer on a Smooth Flat Plate With and Without Heat Transfer. J. Fluid Mech., vol. 18, pt. 1, Jan. 1964, pp. 117-143.

2. Hopkins, Edward J.; and Keener, Earl R.: Study of Surface Pitots for Measuring Turbulent Skin Friction at Supersonic Mach Numbers - Adiabatic Wall. NASA TN D-3478, 1966.

3. Peterson, John B., Jr.: A Comparison of Experimental and Theoretical Results for the Compressible Turbulent-Boundary-Layer Skin Friction With Zero Pressure Gradient. NASA TN D-1795, 1963.

4. Van Driest, E. R.: Problem of Aerodynamic Heating. Aero. Aspects Sessions, Natl. Summer Meeting, IAS, Los Angeles, June 1956. (Also Aeron. Eng. Rev., Oct. 1956, pp. 26-41.)

5. Sommer, S. C.; and Short, B. J.: Free-Flight Measurements of Turbulent Boundary-Layer Skin Friction in the Presence of Severe Aerodynamic Heating at Mach Numbers From 2.8 to 7.0. NACA TN 3391, 1955. (Also J. Aeron. Sci., vol. 23, no. 6, June 1956.)

6. Miles, John B.; and Kim, Jong Hyun: Evaluation of Coles' Turbulent Compressible Boundary-Layer Theory. AIAA J., vol. 6, no. 6, June 1968, pp. 1187-1189.

7. Coles, Donald: The Turbulent Boundary Layer in a Compressible Fluid. Phys. Fluids, vol. 7, no. 9, Sept. 1964, pp. 1403-1423. (Also Rand Rep. R-403-PR, 1962.)

8. Bertram, Mitchel H.; and Neal, Luther, Jr.: Recent Experiments in Hypersonic Turbulent Boundary Layers. NASA TM X-56335, 1965. (Also AGARD Specialists' Meeting on Recent Developments in Boundary-Layer Research, Naples, Italy, May 10-14, 1965.)

9. Bertram, Mitchel H.; Cary, Aubrey M., Jr.; and Whitehead, Allen H., Jr.: Experiments With Hypersonic Turbulent Boundary Layers on Flat Plates and Delta Wings. AGARD Specialists' Meeting on Hypersonic Boundary Layers and Flow Fields, London, England, May 1-3, 1968.

10. Cary, Aubrey M., Jr.: Turbulent Boundary-Layer Heat Transfer and Transition Measurements for Cold-Wall Conditions at Mach 6. AIAA J., vol. 6, no. 5, May 1968, pp. 958-959.

11. Adcock, Jerry B.; Peterson, John B., Jr.; and McRee, Donald I.: Experimental Investigation of a Turbulent Boundary Layer at Mach 6, High Reynolds Numbers, and Zero Heat Transfer. NASA TN D-2907, 1965.

12. Smith, Donald W.; and Walker, John H.: Skin-Friction Measurements in Incompressible Flow. NASA TR R-26, 1959.

13. Hakkinen, Raimo J.: Measurements of Turbulent Skin Friction on a Flat Plate at Transonic Speeds. NACA TN 3486, 1955.

14. Shutts, W. H.; Hartwig, W. H.; and Weiler, J. E.: Final Report on Turbulent Boundary-Layer and Skin-Friction Measurements on a Smooth, Thermally Insulated Flat Plate at Supersonic Speeds. Rep. DRL-364, CM-823, Univ. of Texas Defense Res. Lab., 1955.

15. Stalmach, Charles J., Jr.: Experimental Investigation of the Surface Impact Pressure Probe Method of Measuring Local Skin Friction at Supersonic Speeds. Rep. DRL-410, CR-2675, Univ. of Texas Defense Res. Lab., 1958.

16. Coles, Donald: Measurements in the Boundary Layer on a Smooth Flat Plate in Supersonic Flow III. Rep. 20-71, Jet Propulsion Lab., Calif. Inst. of Tech., 1953.

17. Moore, D. R.; and Harkness, J.: Experimental Investigations of the Compressible Turbulent Boundary Layer at Very High Reynolds Numbers. AIAA J., vol. 3, no. 4, April 1965, pp. 631-638.

18. Matting, Fred W.; Chapman, Dean R.; Nyholm, Jack R.; and Thomas, Andrew G.: Turbulent Skin Friction at High Mach Numbers and Reynolds Numbers in Air and Helium. NASA TR R-82, 1961.

19. Korkegi, Robert H.: Transition Studies and Skin-Friction Measurements on an Insulated Flat Plate at a Mach Number of 5.8. J. Aeron. Sci., vol. 23, no. 2, Feb. 1956, pp. 97-107, 192.

20. Neal, Luther, Jr.: A Study of the Pressure, Heat Transfer, and Skin Friction on Sharp and Blunt Flat Plates at Mach 6.8. NASA TN D-3312, 1966.

21. Wallace, J. E.; and McLaughlin, E. J.: Experimental Investigations of
     Hypersonic, Turbulent Flow and Laminar, Leeward-Side Flow on Flat
     Plates. Tech. Rep. AFFDL-TR-66-63, Vol. I, Cornell Aeronautical Lab.,
     July 1966.

22. Seiff, Alvin; and Short, Barbara J.: An Investigation of Supersonic
     Turbulent Boundary Layers on Slender Bodies of Revolution in Free
     Flight by Use of a Mach-Zehnder Interferometer and Shadowgraphs.
     NACA TN 4364, 1958.

23. Wallace, J. E.: Hypersonic Turbulent Boundary-Layer Studies at Cold Wall
     Conditions. Proceedings of the 1967 Heat Transfer and Fluid Mechanics
     Institute, Univ. of Calif., San Diego, June 19-21, 1967, pp. 427-451.

24. Wallace, J. E.: Hypersonic Turbulent Boundary- Layer Measurements Using
     an Electron Beam. Tech. Rep. CAL AN-2112-Y-1, Cornell Aeronautical
     Lab., Aug. 1968.

25. Van Driest, E. R.: Investigation of Laminar Boundary Layer in Compres-
     sible Fluids Using the Crocco Method. NACA TN 2597, 1952.

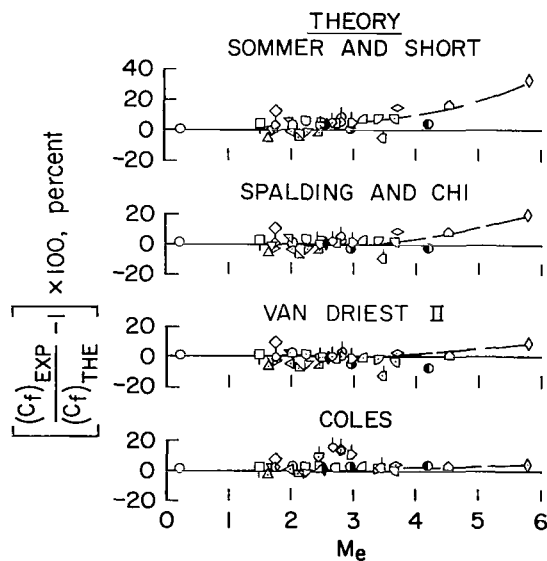TABLE I.- SKIN-FRICTION DATA FOR FLAT PLATES IN THE AMES 3.5-FOOT WIND TUNNEL

M_e	$(\rho_e U_e/\mu_e) \times 10^{-6}$, ft^{-1}	$(R_{e,\theta}) \times 10^{-3}$	$T_{t,e}$, °R	T_w, °R	T_e, °R	T_w/T_{aw}	$(C_f) \times 10^3$	Boundary-layer trips	Source
6.5	1.70	2.26	1850	583	205	0.34	1.57	Off	
	2.62	4.56	1960	587	218	.32	1.22	On	
	1.64	3.30	1410	551	153	.43	1.25	On	
	2.37	5.90	1477	564	161	.42	1.20	On	Hopkins and
	1.49	2.39	1474	559	160	.41	1.52	Off	Keener,
	2.82	3.82	1376	561	149	.45	1.23	Off	stationary
	1.26	2.19	1158	537	124	.51	1.41	On	flat plate
	1.81	3.89	1250	543	130	.50	1.35	On	
	4.01	8.33	1240	572	133	.51	1.00	On	
	4.07	6.42	1231	572	132	.51	1.06	Off	
7.4	2.39	3.01	1963	560	172	.31	1.26	Off	Keener and
7.4	4.53	5.67	1983	573	172	.31	1.08	Off	Polek, injected flat plate

TABLE II.- SKIN-FRICTION DATA FOR SIDE WALL OF THE AMES 3.5-FOOT WIND TUNNEL

M_e	$(\rho_e U_e/\mu_e) \times 10^{-6}$, ft^{-1}	$(R_{e,\theta}) \times 10^{-3}$	$T_{t,e}$, °R	T_w, °R	T_e, °R	T_w/T_{aw}	$(C_f) \times 10^4$
7.4	2.95	52.4	1359	543	114	0.44	6.84
	3.86	56.4	1340	555	112	.46	6.50
	1.16	20.5	1273	544	109	.47	7.14
	1.97	40.2	1250	552	105	.49	6.76
	2.73	48.1	1404	558	118	.44	6.70
	4.01	62.6	1328	568	111	.47	6.30
	.91	18.7	1453	554	125	.42	8.08
	1.88	31.7	1363	567	113	.46	7.26
	.69	16.4	1595	546	133	.39	8.86
	1.44	28.4	1561	558	129	.40	7.82
	2.09	52.6	1637	557	139	.37	7.33
	2.98	53.0	1564	568	132	.40	7.12
	.71	21.1	1686	552	146	.35	9.12
	1.34	30.1	1685	562	144	.36	7.97
	.63	13.2	1812	554	158	.33	9.45
	1.23	33.0	1795	564	155	.34	8.43
	1.66	42.1	1879	558	162	.32	8.13

SYMBOL	M_e	$(R_{e,\theta}) \times 10^{-3}$	SOURCE
○	0.22	7	SMITH AND WALKER, REF. 12
⊡	1.50	2	HAKKINEN, REF. 13
△	1.63	12	SHUTTS et al., REF. 14
▽	1.68	20	↓
▷	1.73	13	
◇	1.75	2	HAKKINEN, REF. 13
◇	1.75	8	STALMACH, REF. 15
◁	1.97	6	COLES, REF. 16
◁	2.00	13	SHUTTS et al., REF. 14
◻	2.01	8	STALMACH, REF. 15
◺	2.11	14	SHUTTS et al., REF. 14
◻	2.23	7	STALMACH, REF. 15
▽	2.25	13	SHUTTS et al., REF. 14
◿	2.46	12	↓
◊	2.46	68	HOPKINS AND KEENER, REF. 2
◻	2.49	7	STALMACH, REF. 15
◆	2.56	6	COLES, REF. 16
◇	2.67	690	MOORE AND HARKNESS, REF. 17
◈	2.80	360	
◈	2.80	81	↓
◻	2.72	7	STALMACH, REF. 15
◻	2.95	7	
◕	2.95	15	MATTING et al., REF. 18
◔	2.96	61	HOPKINS AND KEENER, REF. 2
◁	3.16	7	STALMACH, REF. 15
▽	3.39	7	↓
◊	3.45	56	HOPKINS AND KEENER, REF. 2
◻	3.67	6	STALMACH, REF. 15
◇	3.69	5	COLES, REF. 16
◐	4.20	13	MATTING et al., REF. 18
△	4.53	5	COLES, REF. 16
◇	5.79	3	KORKEGI, REF. 19

(a) Data identification.

THEORY

SOMMER AND SHORT

SPALDING AND CHI

VAN DRIEST II

COLES

$\left[\dfrac{(C_f)_{EXP}}{(C_f)_{THE}} - 1\right] \times 100$, percent

M_e
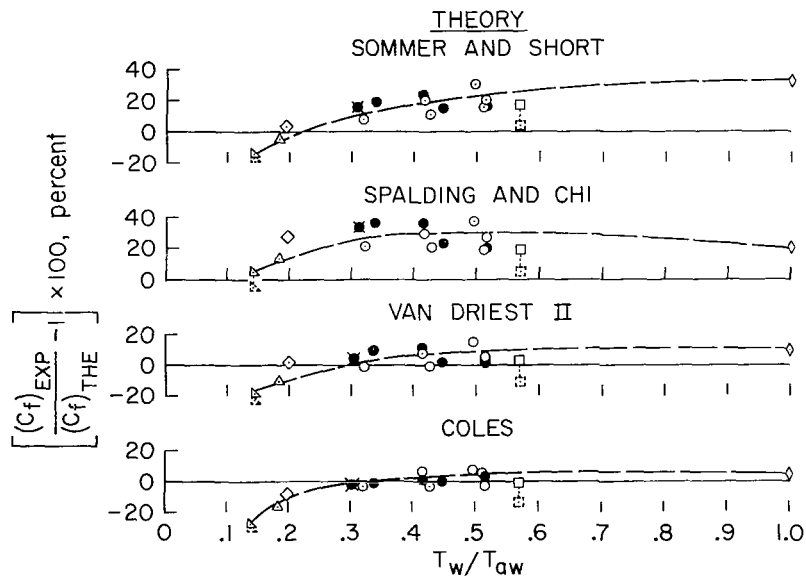
(b) Comparison of data with theory.

Figure 1.- Adiabatic-wall skin friction; C_f and $R_{e,\theta}$ directly measured.

SYM	M_e	B.L. TRIPS	$(R_{e,\theta}) \times 10^{-3}$	$(R_{e,x}) \times 10^{-6}$	SOURCE
o	6.5	ON	5		AMES 3.5 ft W.T.* (HOPKINS AND KEENER, UNPUBLISHED)
●	6.5	OFF	4		
✕	7.4	OFF	4		(KEENER AND POLEK, UNPUBLISHED)
◻	6.8	OFF		3	NEAL, REF. 20**
◌	6.8	OFF		2	
△	7.0	ON		1	SOMMER AND SHORT, REF. 5
◇	5.6	ON		8	
◺	7.4	OFF		18	WALLACE AND McLAUGHLIN, REF. 21**
◺	7.4	OFF		13	
◊	5.8	ON	3		KORKEGI, REF. 19

* THE TWO DIFFERENT MODELS CAN BE IDENTIFIED AS STATIONARY (o,●) AND INJECTED MODEL (✕)

** REGULAR SYMBOLS REPRESENT VIRTUAL ORIGIN CALCULATED FROM $(x_L)(c_{F,L}) = (x_T)(c_{F,T})$ DASHED SYMBOLS REPRESENT VIRTUAL ORIGIN AT $c_{h,MAX}$
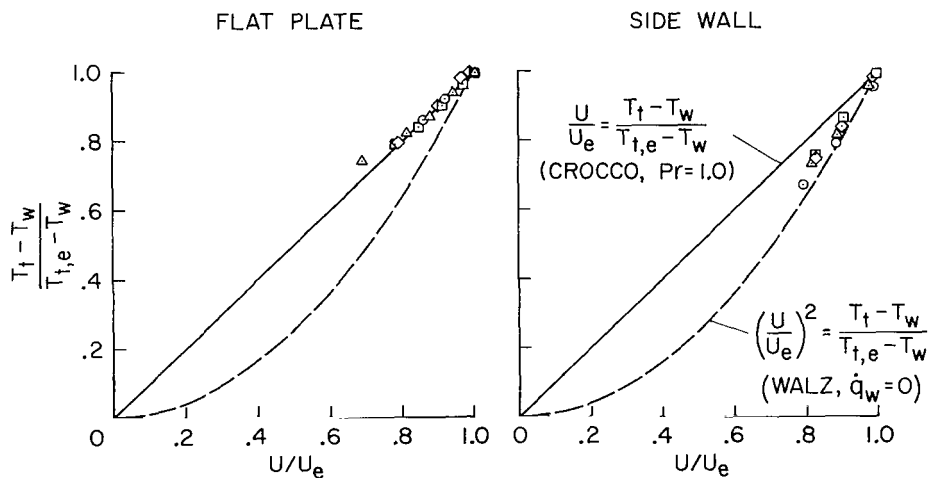
(a) Data identification.

(b) Comparison of data with theory.

Figure 2.- Nonadiabatic-wall skin friction for flat plates; C_f directly measured.

FLAT PLATE

SYM	M_e	$(R_{e,\theta}) \times 10^{-3}$	$T_w/T_{t,e}$	$T_{t,e}$, °R	B.L. TRIPS
○	6.5	2.26	0.315	1850	OFF
□	6.5	4.56	.300	1960	ON
◇	6.5	3.30	.391	1410	ON
△	6.5	5.90	.382	1477	ON

SIDE WALL

SYM	M_e	$(R_{e,\theta}) \times 10^{-3}$	$T_w/T_{t,e}$	$T_{t,e}$, °R	
○	7.4	40.2	0.442	1250	
□	7.4	52.4	.400	1359	
◇	7.4	53.0	.363	1564	
△	7.4	47.5	.304	1881	

(a) Data identification.

FLAT PLATE   SIDE WALL

$$\frac{U}{U_e} = \frac{T_t - T_w}{T_{t,e} - T_w} \quad (\text{CROCCO, Pr}=1.0)$$

$$\left(\frac{U}{U_e}\right)^2 = \frac{T_t - T_w}{T_{t,e} - T_w} \quad (\text{WALZ}, \dot{q}_w = 0)$$
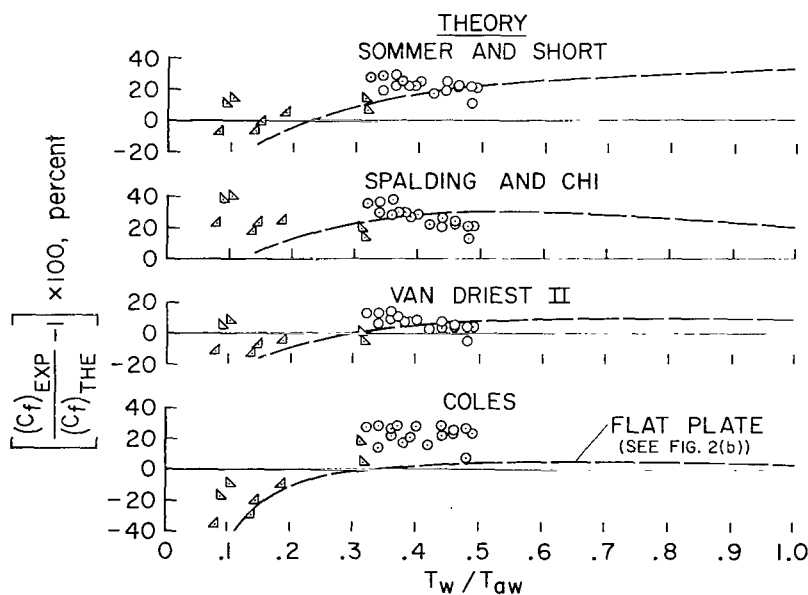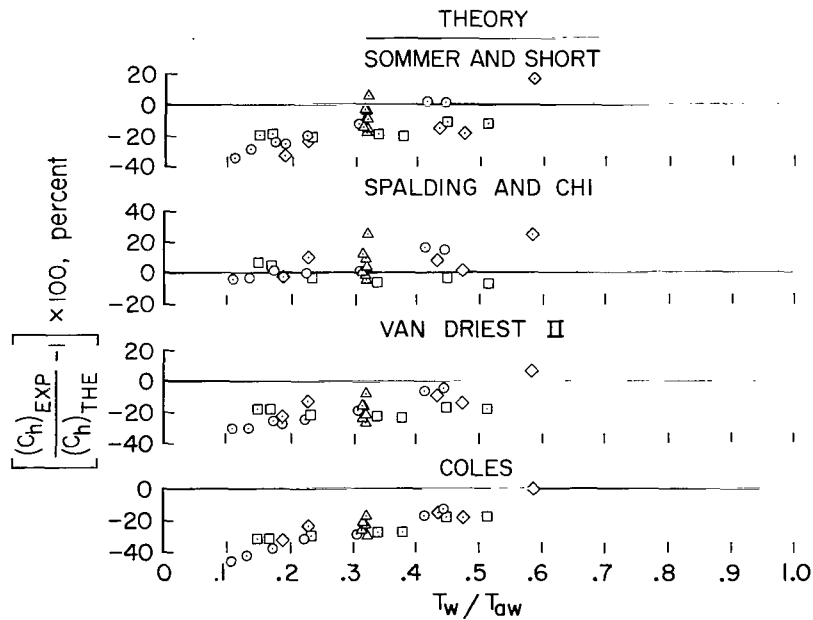
(b) Comparison of data with theory.

Figure 3.- Temperature-velocity profiles measured in the Ames 3.5-Foot Wind Tunnel by Hopkins and Keener; nonadiabatic wall.

21

SYMBOL	M_e	$(R_{e,\theta}) \times 10^{-3}$	SOURCE
○	7.4	37	HOPKINS AND KEENER, UNPUBLISHED
◁	7.5	44	WALLACE, REF. 23*
◁	8.6	6	WALLACE, REF. 24

* DATA RECALCULATED WITH A QUADRATIC TEMPERATURE DISTRIBUTION ASSUMED

(a) Data identification.

(b) Comparison of data with theory.

Figure 4.- Nonadiabatic-wall skin friction for wind-tunnel walls; C_f and $R_{e,\theta}$ directly measured.
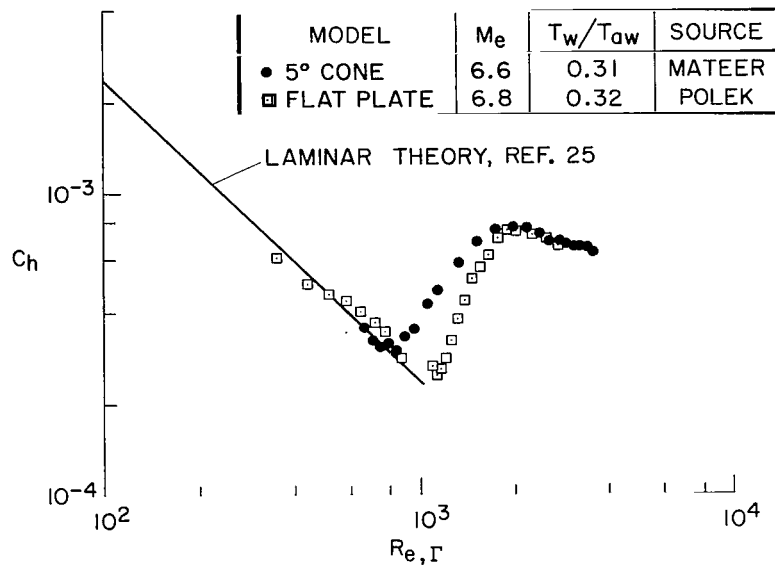
Figure 5.- Stanton number variation with energy-thickness Reynolds number; Ames 3.5-Foot Wind Tunnel.

SYM	M_e	$(R_{e,\Gamma}) \times 10^{-3}$	MODEL	SOURCE
○	6.6	4	5° CONE	MATEER, UNPUBLISHED
□	4.9	4	15° CONE	
◇	5.0	4	5° CONE	
△	7.4–6.8	5	FLAT PLATE (α = 0 AND 3.1°)	POLEK, UNPUBLISHED

(a) Data identification.

(b) Comparison of data with theory; $C_h/(C_f/2)$ = 1.16 and r = 0.9.

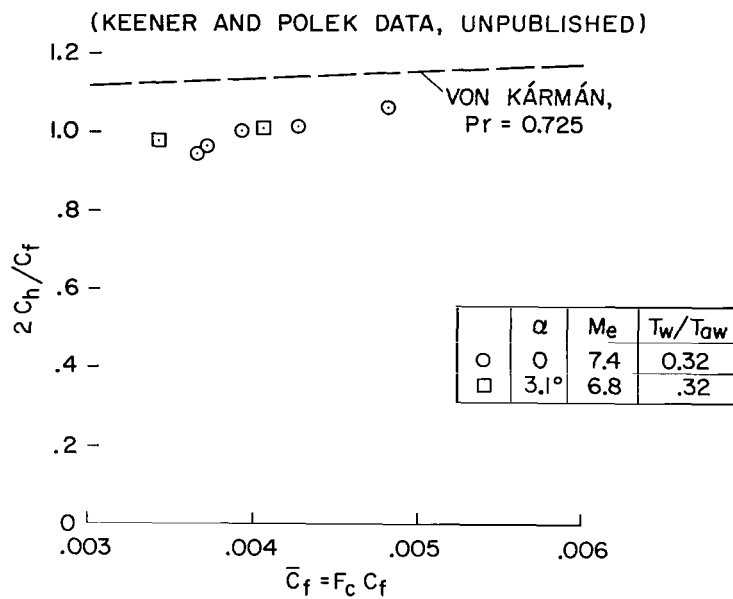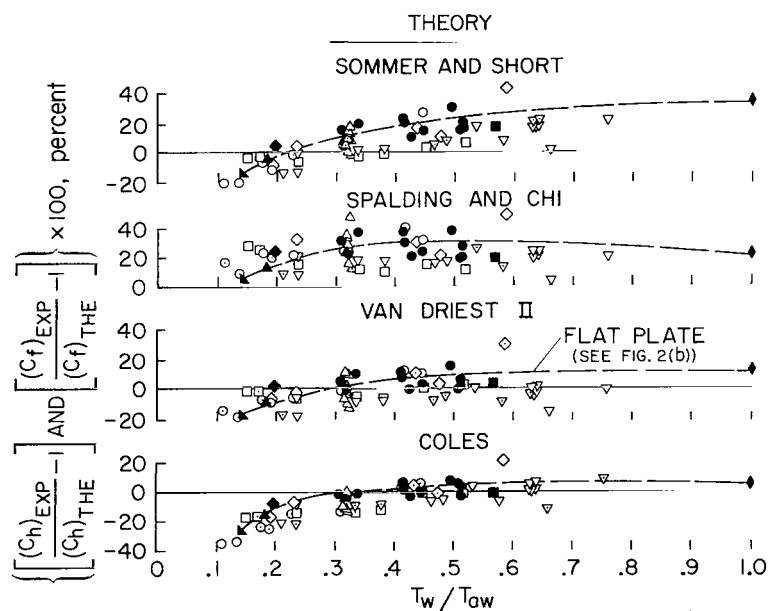Figure 6.- Nonadiabatic-wall heat-transfer data; Ames 3.5-Foot Wind Tunnel.

24

Figure 7.- Reynolds analogy factors measured for a flat plate; Ames 3.5-Foot Wind Tunnel; r = 0.9.

SYM	M_e	MODEL	$(R_{e,\theta}) \times 10^{-3}$ OR $(R_{e,r}) \times 10^{-3}$	$(R_{e,x}) \times 10^{-6}$	SOURCE
●	6.5	FLAT PLATE	5		HOPKINS AND KEENER, UNPUBLISHED
■	6.8	FLAT PLATE		3	NEAL, REF. 20
▲	7.0	CYLINDER		1	SOMMER AND SHORT, REF. 5
◆	5.6	CYLINDER		8	
◣	7.4	FLAT PLATE		18	WALLACE AND McLAUGHLIN, REF. 21
◆	5.8	FLAT PLATE	3		KORKEGI, REF. 19
○	6.6	CONE	4		
□	4.9	CONE	4		MATEER, UNPUBLISHED
◇	5.0	CONE	4		
△	6.8–7.4	FLAT PLATE	5		POLEK, UNPUBLISHED
▽	6.0	FLAT PLATE	5		CARY, REF. 10

TYPE DATA
   OPEN SYMBOL – HEAT TRANSFER
   SOLID SYMBOL – SKIN FRICTION

(a) Data identification.

(b) Comparison of data with theory; $C_h/(C_f/2) = 1.0$ and $r = 0.9$.

Figure 8.– Nonadiabatic-wall skin-friction and heat-transfer data.

"The aeronautical and space activities of the United States shall be
conducted so as to contribute . . . to the expansion of human knowl-
edge of phenomena in the atmosphere and space. The Administration
shall provide for the widest practicable and appropriate dissemination
of information concerning its activities and the results thereof."

— NATIONAL AERONAUTICS AND SPACE ACT OF 1958

NASA SCIENTIFIC AND TECHNICAL PUBLICATIONS

TECHNICAL REPORTS: Scientific and
technical information considered important,
complete, and a lasting contribution to existing
knowledge.

TECHNICAL NOTES: Information less broad
in scope but nevertheless of importance as a
contribution to existing knowledge.

TECHNICAL MEMORANDUMS:
Information receiving limited distribution
because of preliminary data, security classifica-
tion, or other reasons.

CONTRACTOR REPORTS: Scientific and
technical information generated under a NASA
contract or grant and considered an important
contribution to existing knowledge.

TECHNICAL TRANSLATIONS: Information
published in a foreign language considered
to merit NASA distribution in English.

SPECIAL PUBLICATIONS: Information
derived from or of value to NASA activities.
Publications include conference proceedings,
monographs, data compilations, handbooks,
sourcebooks, and special bibliographies.

TECHNOLOGY UTILIZATION
PUBLICATIONS: Information on technology
used by NASA that may be of particular
interest in commercial and other non-aerospace
applications. Publications include Tech Briefs,
Technology Utilization Reports and Notes,
and Technology Surveys.

Details on the availability of these publications may be obtained from:

SCIENTIFIC AND TECHNICAL INFORMATION DIVISION

NATIONAL AERONAUTICS AND SPACE ADMINISTRATION
Washington, D.C. 20546